

# Study Of Maximum Power Point Tracking (MPPT) In PV Systems

Fathy M. Mustafa<sup>1</sup>, M. Elzalik<sup>2</sup>, R. Mostafa<sup>3</sup>

<sup>1</sup>Electronics and Communications Engineering Department, Beni-suef University, Egypt

<sup>2</sup>Process Control Technology Department, Faculty of industrial Education, Beni-suef University, Egypt

<sup>3</sup>Professor, Head of Process Control Technology Department, Beni-suef University, Egypt

**Abstract**—the performance of a photovoltaic (PV) module is mostly affected by array configuration, irradiance and module temperature it is important to understand the relationship between these effects and the output power of the PV array. In this paper, a new method to track the global MPP is presented, which is based on using PIC microcontroller which controlling a DC-DC converter connected at the PV array output, such that it behaves as a constant input-power load. I-V and P-V characteristics curves of simulation match the measurements from outdoor experimental under the condition of uniform irradiance; both simulation and experiment show the output power of a PV array. Perturb and Observe (P&O) and Incremental conductance (INC). The experiments show that the proposed model has good predictability in the general behaviors of MPPT under the conditions of both non uniform and uniform irradiance.

**Keywords:** MPPT, PV array, DC-DC converter, PIC microcontroller, Perturb and Observe, Incremental conductance.

## 1. Introduction

Due to increasing demand for electricity, and limited stock of high-traditional sources of prices (such as coal, oil, etc.), and photovoltaic (PV) energy becomes promising as is the case everywhere, which is freely available, environmentally friendly, and has a lower operation and maintenance costs substitute [1]. Therefore, it seems that the demand for PV generation systems to increase for each of the independent media and grid-connected PV systems. So, which it is the maximum power point tracking (MPPT) technology effectively is necessary, which is expected to follow the MPP in all environmental conditions and then impose a PV system to work at that point MPP. [1].

Among those techniques, and "confusion and control" (P & O) and scheme (INC) scheme additional disposal are the most common

because of the ease of implementation. The main drawback of these methods is that they can only follow a maximum of one, which is absent when partially shaded solar panels. The reason is that these methods rely on the "hill climb" the principle of OP next move in the direction that increases the strength. If PV (or PI) feature is not unimodal, you can only reach these methods successfully at a local maximum [2]. In typical photovoltaic (PV) installations, PV arrays are formed by connecting multiple PV modules in various configurations (ie series, parallel, parallel, series, etc.). It has been exceeded diode or bypass switch in parallel with each unit PV solar cells to protect against the effects of the deterioration of efficiency and hot plug failure. Under the conditions of a unified solar rays between individual PV modules, and voltage power (PV) feature of the PV group exhibits a unique operating point of its kind where the PV power generation as much as possible (maximum power point, MPP) [3]. And the increasing adoption of Maximum Power Point Tracking (MPPT) multiphase DC adapters, DC in PV systems, they provide improved dynamic performance and steady-state with higher reliability compared with traditional topology [4].

PV cells suffer from low efficiency of approximately 10% to 40%. Moreover, the maximum power output of photovoltaic cells degrades under changing weather conditions. To maximize the efficiency of PV energy harvest, and maximum power point tracking (MPPT) technology, which enables the operating point of the PV cells to track the maximum power point (MPP), has been implemented in the PV energy harvesters [5]. Power output of photovoltaic panels (PPV) depends on the weather conditions (solar radiation, temperature and conditions of shading level.), And load [6]. PV panel has a non-linear characteristic, the power to have the

maximum Power Point (MPP) work at a certain point, with coordinates VMPP effort and integrated planning for the current missions. Since the MPP depends on the weather conditions, and it is never constant over time. It is necessary to operate the system in its MPP. It is usually implemented Maximum Power Point Tracking (MPPT) algorithms using the power of the electronic communication between the PV panel and the energy storage device or pregnancy should be used to track changes in [7].

In the present paper, The INC MPPT algorithm and the P&O algorithm are implemented using a low-cost, low-power consumption PIC microcontroller, which controls a buck DC-DC converter for stand-alone PV power system applications. The voltage, current, power and duty cycle are measured and send every sampling period to a computer to study the actual performance of MPPT algorithms at different step values of perturbation to determine the range of optimal step in the mentioned algorithms. The P-V and I-V characteristics of PV module are measured in actual environmental conditions and plotted using MATLAB program to determine Vmpp, Impp and Pmpp which vary with irradiance, temperature, spectrum and other conditions.

### 2. Modeling the PV Array

The difference between an ideal PV cell and practical PV devices are the presence of resistances (both series and parallel). Solar cell equivalent circuit, where I is the current through the circuit, V is the voltage in the circuit, Rs is the series resistance in the PV circuit, Rp is the parallel resistance in the PV circuit, Io is the reverse saturation current of the diode. The Figure 1 shows an ideal solar PV cell equivalent circuit which mathematically describes the I-V characteristics of the PV circuit given by, [8], [9], [10], [11].

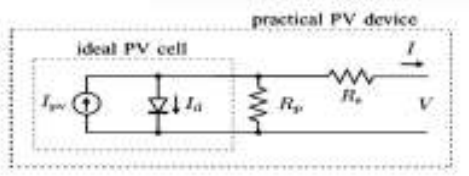


Figure 1. Circuit of a Practical PV Solar Cell [11].

$$I = I_{ph} - I_d \left[ \exp\left(\frac{qV_b}{akT}\right) - 1 \right] \quad (1)$$

Where  $I_{ph}$  is the current solar cell generates at optimum conditions.

The (1) does not represent the I-V characteristics of the PV cell array, as practical array consists many components and thus (1) requires additional parameters like the series resistance, represented as in (2),

$$I = I_{ph} - I_d \left[ \exp\left(\frac{V + IR_s}{aV_b}\right) - 1 \right] - \frac{V + IR_s}{R_p} \quad (2)$$

Where  $R_s$  is the series resistance,  $R_p$  is the resistance in parallel of the solar cell array, ‘a’ is the diode ideality constant and,  $V_b = \frac{kTN_{ser}}{q}$ , where  $V_b$  is the thermal voltage of the solar cell array with  $N_{ser}$  connected in series. Due to the affect of the temperature and linearity of the solar irradiation resulting in the generation of the current, is,

$$I_{ph} = I_{ph,nom} + K_{cur}(T - T_{nom}) + \left(\frac{G}{G_{nom}}\right) \quad (3)$$

Where  $I_{ph,nom}$  is the current generated in solar cell circuit at nominal conditions (when temperature is 25° Celsius and irradiance of 1000 W/m².)

$K$  is the Boltzman’s constant ( $1.381 \times 10^{-23}$  J/K) and  $q$  is the electron charge ( $1.602 \times 10^{-19}$  C).

$T$  is actual temperature and  $T_{nom}$  is the nominal temperature,  $G$  is the actual irradiation and  $G_{nom}$  is the nominal irradiation (usually 1000 W/m²). The diode saturation current  $I_o$  and its dependence on temperature can be given by,

$$I_d = I_{o,nom} + \exp\left(\frac{T_{nom}}{T}\right)^3 \exp\left[\frac{qE_g}{akT} \left(\frac{1}{T} - \frac{1}{T_{nom}}\right)\right] \quad (4)$$

Here  $I_{o,nom}$  is the diode saturation current at nominal conditions and  $E_g$  is the band gap energy of the semiconductor which is usually taken as 1.12eV. The value of the  $I_{o,nom}$  can be found out from,

$$I_{o,nom} = \frac{I_{sc}}{\exp\left(\frac{V_{oc}}{aV_b}\right) - 1} \quad (5)$$

The previous equation gives the output power  $P$  of the cell is:

$$p = V \times I \quad (6)$$

The value of the diode ideality constant can be randomly selected within the range of  $0 \leq a \leq 2$ . But for the calculation in this research work the value of ‘a’ is taken as 1.528. For modeling purposes, we use the module GP50W. The PV module is made up of multi-crystalline silicon having 40 solar cells in series connection. The PV module provides a maximum power of 50 watts. Table 1 shows the Electrical specifications of the PV module.

Electrical Characteristics (module GP50W)	
Maximum Power ( $P_{Maxp}$ )	50 W
Voltage at $P_{Maxp}$ ( $V_{Maxp}$ )	16.7 V
Current at $P_{Maxp}$ ( $I_{Maxp}$ )	3 A
Open-circuit voltage ( $V_{oc}$ )	21.5 V
Short-circuit current ( $I_{sc}$ )	3.3 A
Temperature coefficient of $I_{sc}$ , $K_{cur}$	$0.65 \times 10^{-3}$
Temperature coefficient of $V_{oc}$ , $K_{volt}$	3.3
NOCT	47°

Table 1. The PV array electrical characteristics

The electrical characteristics are simulated with the MATLAB model for GP50 PV module. These characteristics depend on external factors including temperature and solar irradiation level. The effects of solar irradiation and temperature on the characteristics of the PV module are depicted in figures 2, 3, 4 and 5.

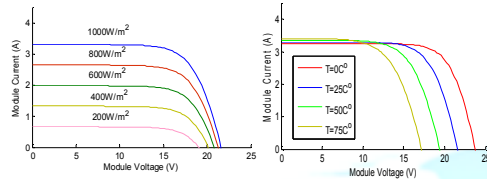


Figure 2. I-V characteristics of the PV module under different solar irradiation levels.

Figure 3. I-V characteristics of the PV module at different surface temperatures.

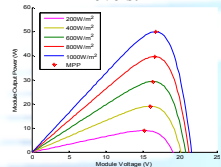


Figure 4. P-V characteristics of the PV module under different solar irradiation levels.

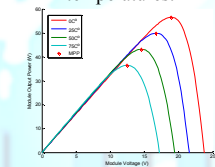


Figure 5. P-V characteristics of the PV module at different surface temperatures.

### 3. Maximum Power Point Tracking (MPPT) Techniques

In order to capture the maximum power available from the PV array, a Maximum Power Point Tracker (MPPT) is required. Several algorithms can be used in order to implement the MPPT; but perturb and observe (P&O) and Incremental Conductance (INC) techniques are widely used, because they are especially for low-cost implementations [12].

#### 3.1 Perturb and Observe method

Perturb and observe (P&O) method is the most common for its simplicity, ease of implementation, and good performance. Small increment or decrement of perturbed voltage  $M$  has been instructed by the algorithm to the PV module operating voltage. The tracking process is followed by observing the array output power and subsequently P&O determines the further action either to increase or decrease the array operating voltage by  $M$ . Figure 6 shows the operation flowchart of the P&O MPPT algorithm, where the parameter  $M$  is the scaling factor, tuned at design time to scale the step size. [13].

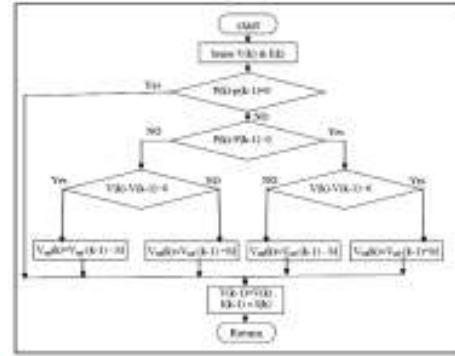


Figure 6. Flowchart of P&O method

The major drawbacks of P&O algorithm are presence of oscillations around the MPP in steady state operation and occasional deviation from the maximum operating point in case of rapidly changing atmospheric conditions, such as broken clouds. Also, correct perturbation size is important in providing good performance in both dynamic and steady-state response. There are several variations of the basic P&O that have been proposed to minimize these drawbacks. These include using dynamically adjusting the magnitude of the perturbation  $M$  of the PV operating point and an average of several samples of the array power [12].

#### 3.1.1 Improved P&O techniques for rapidly changing irradiance (dp-P&O)

The method performs an additional measurement of power in the middle of the MPPT sampling period without any perturbation, and based on these measurements, it calculates the change of power due to the varying irradiance. The resulting “ $dP$ ” reflects the changes due to the perturbation of the MPPT method as show in figure 7. Using the below calculation in the flowchart of the dp-P&O method, as show in figure 8 can be avoided the confusion of the MPPT due to the rapidly changing irradiance [13], [14].

Assuming that the rate of change in the irradiance is constant over one sampling period of the MPPT, the  $dP$  caused purely by the MPPT command can be calculated as:

$$dP = dP_1 - dP_2 = (P_x - P_k) - (P_{k+1} - P_x) = 2P_x - P_{k+1} - P_k \quad (7)$$

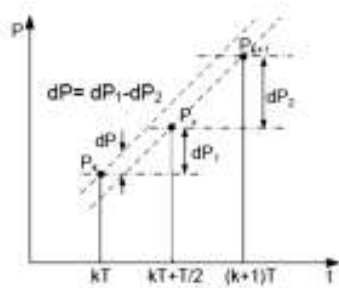


Figure 7. Measurement of the power between two MPPT sampling instances

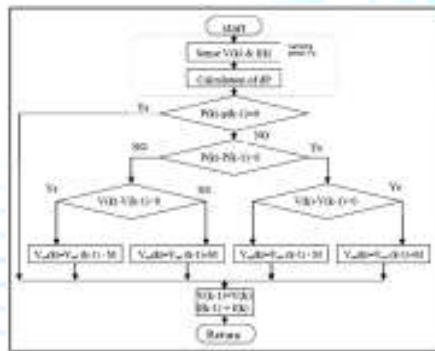


Figure 8. The flowchart of the dp-P&O method.

### 3.1.2 Variable step size of perturbation and dP-P&O Algorithm (VM-dP-P&O Algorithm)

In this algorithm is margin between variable step size of perturbation P&O Algorithm and dP-P&O Algorithm. This Algorithm is called (VM-dP-P&O Algorithm), Fig.9 show The flowchart of the proposed VM-dP-P&O Algorithm.

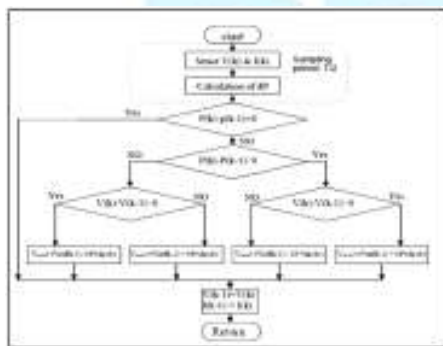


Figure 9. The flowchart of the proposed VM-dP-P&O Algorithm.

### 3.2 Incremental conductance (INC) method

This is based on the fact that the slope of the PV array power versus voltage curve is zero at the MPP. This

method has been proposed to improve the limitations of the P&O algorithm by improving the tracking accuracy and dynamic performance under rapidly varying conditions [15]. Flowchart of the INC MPPT method is shown in Figure 10, by using the PV array's incremental conductance to compute the sign of  $dP/dV$  without a perturbation. It does this using an expression derived from the condition that, at the MPP,  $dP/dV = 0$ . Beginning with this condition, it is possible to show that, at the MPP  $dI/dV = -I/V$ . Thus, incremental conductance can determine that the MPPT has reached the MPP and stop perturbing the operating point. If this condition is not met, the direction in which the MPPT operating point must be perturbed can be calculated using the relationship between  $dI/dV$  and  $-I/V$ . This relationship is derived from the fact that  $dP/dV$  is negative when the MPPT is to the right of the MPP and positive when it is to the left of the MPP [16].

The advantage of incremental conductance over the perturb-and-observe algorithm is actually calculation of the direction in which to perturb the array's operating point to reach the MPP, can determination when it has actually reached the MPP. Thus, under rapidly changing conditions, it can track rapidly increasing and decreasing irradiance conditions with higher accuracy than perturb and observe. However, null value of the slope of the PV array power versus voltage curve seldom occurs due to the resolution of digital implementation. Although the INC method is a little more complicated compared with the P&O algorithm, it can be easily implemented due to the advancements of digital signal processors (DSPs) [17].

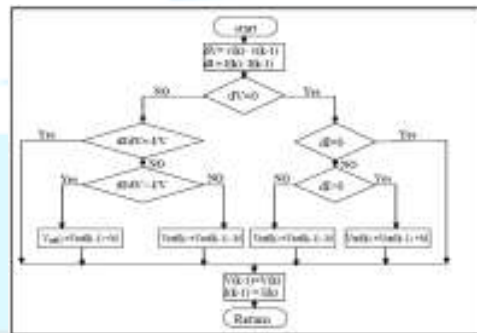


Figure 10. The flowchart of the INC MPPT algorithm.

### 4. Measurement of PV MPPT Performance

The actual operating voltage and current of the PV array are readily measured but, it is not easy to determine  $V_{max}$  and  $I_{max}$  which vary with irradiance, temperature, spectrum and other conditions. There are two methods to determine  $V_{max}$  and  $I_{max}$  to measure the MPPT performance, which are divided into laboratory (indoor) and field (outdoor) measurements [18]. In laboratory measurements, a PV array simulator is necessary to generate DC power with the I-V curve characteristic of a PV array. The simulator

must be able to simulate an array under a variety of conditions (including different fill factors signifying different cell technologies) with satisfactory static accuracy. In the other hand, the outdoor measurements have the advantage that actual MPPT behavior will be observed with the real PV array avoiding potentially unrealistic interactions between the MPPT and PV array simulator. Obtaining the necessary range of parameters outdoors requires co-operative weather as well as access to a variety of PV technologies.

Figure 11, shows the block diagram of the proposed control and measurement circuit of MPPT. The MPP and PV characteristics are determined in Outdoor measurements using switching between MPPT and I-V Tracer. The principle of I-V Tracer is depending on two methods to measure I-V and P-V characteristic and determine MPP. The first method is depending on setting the selector switch to trace 60W variable resistance; the voltage and current are measured at different values of variable resistance under normal conditions. The second method is depending on change the value of duty cycle from zero to one by step 0.02 every one second and measure voltage and current at different values of duty cycle. To give accurate results, it is essential that the ambient conditions do not change significantly between the I-V curve trace and the normal MPPT operation. To ensure that, no rapid change in the weather conditions, the measurements are executed in a short time.

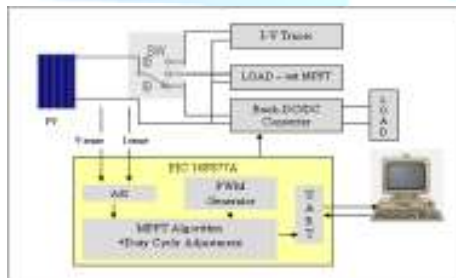


Figure 11. Block diagram of proposed control and measurement circuit of MPPT

The circuit is divided into two basic parts, buck DC/DC converter, and the control and measurement circuit using microcontroller. A DC-DC converter acts as an interface between the load and the solar PV module to detect and track the MPP produced by the PV module, under different atmospheric conditions and connected load. Three basic DC-DC converter topologies are used in PV systems: step down (buck), step up (boost) and step down converters [19],[20]. The type of converter is determined during the design phase according to the required load power and voltage. If it is possible to connect several series modules to get high array voltage and low array current; buck converter is used.

PIC reading the voltage and current of the solar panels through the A/D converter and calculates the solar watts generated and adjusting the duty cycle of the

DC/DC converter to track the MPP According to the algorithm on the memory

Table 2 shows the different tests of MPPT algorithms at different value step size of perturbation M.

Algorithms	Different tests of MPPT algorithms with different value step size of perturbation M.			
	M1	M2	M3	M4
P&O-1(classic P&O)	0.01	0.001	0.05	0.005
P&O-3(dP-P7O)	0.01	0.001	0.05	0.005
INC (Inc)	0.01	0.001	0.05	0.005

Table 2. Different tests of MPPT algorithms with different value step size of perturbation M.

All testes are executed in sunny day, the irradiance level changes gradually since there is no influence of cloud.

## 5. Results and experimental evaluation

In this section we show P-V and I-V characteristic of PV module measured and plotted, also we disseminated and show the output power at direct connection without MPPT and the output power after using MPPT at different step values of perturbation M1, M2, M3 and M4 in P&O-1, P&O-3 and INC tests. For each test of PV module measured and plotted using MATLAB

### 5.1 MPPT measured at the different tests

Table 3, shows the values of MPP measured at different tests to determine MPP before each test.

Algorithms	Maximum Power at different tests of MPPT algorithms with different value step size of perturbation M			
	M1	M2	M3	M4
	P <sub>MAX</sub>	P <sub>MAX</sub>	P <sub>MAX</sub>	P <sub>MAX</sub>
P&O-1(classic P&O)	35.37 453	34.71 214	35.47 362	35.49 734
P&O-3(dP-P&O)	35.02 486	36.07 561	35.72 953	36.52 983
INC (Inc)	37.47 989	37.24 310	36.17 443	35.62 776

Table 3. MPPT at different tests.

#### 5.1.1 The P-V and I-V characteristic for each test of PV module

Figures 12 to 14 shows P-V and I-V characteristic for each test of PV module measured and plotted using MATLAB.

##### A. P&O-1 test

Figure 12; show P-V and I-V of PV module

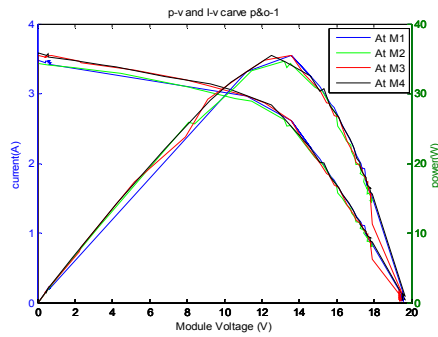


Figure 12, P-V and I-V characteristic of PV module at P&O-1 test.

In this test we obtained the maximum power equal to  $34.71214 W$  at step value of perturbation M4.

**B. P&O-3 test**

Figure 13, show P-V and I-V of PV module

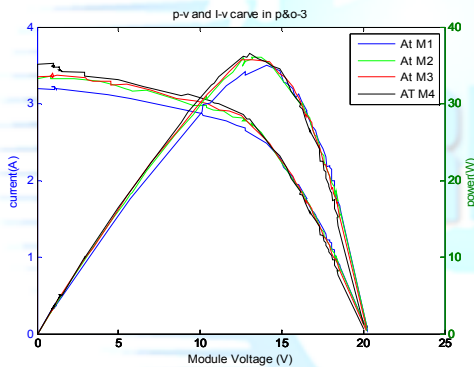


Figure 13, P-V and I-V characteristic of PV module at P&O-3 test.

We obtained the maximum power equal to  $36.52983 W$  at step value of perturbation M4.

**A. INC test**

Figure 14, show P-V and I-V of PV module

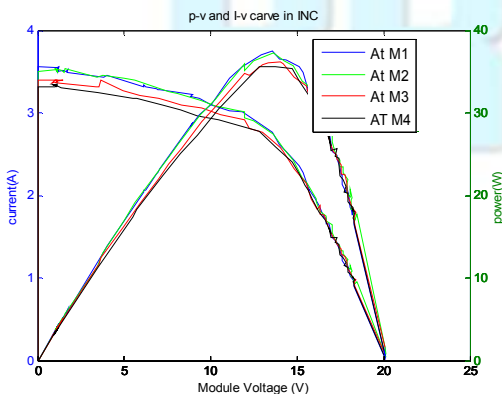


Figure 14, P-V and I-V characteristic of PV module at INC test

Form figure we get maximum power equal to  $37.47989 W$  at step value of perturbation M1.

**5.1.2 The output power without MPPT and with MPPT**

In this part we shows the output power of all tests The output power at direct connection without MPPT and the output power after using MPPT at different step values of perturbation M1, M2, M3 and M4 in P&O-1, P&O-3 and INC tests are shown in figures below.

**A. The output power at P&O-1 test**

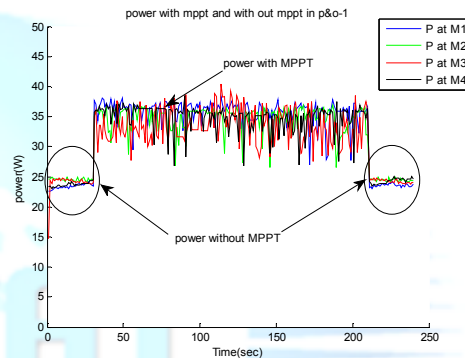


Figure 15. The output power at P&O-1 test

From figure 15, we get the output power in case of MPPT is larger than the output power without MPPT, also at M4 we get large output power ( $P_{MAX} = 35.49734 W$ ) but at M2 get smaller output power ( $P_{MAX} = 34.71214 W$ ). Also we can calculate the average output power without MPPT, the average power with MPPT and the improvement in output power at different step values of perturbation M1, M2, M3 and M4, according to table 4.

P&O-1	M1 0.01	M2 0.001	M3 0.05	M4 0.005
Average power without MPPT	23.6237 5	24.4210	23.9241 0	24.0302 9
Average power with MPPT	35.8575 9	34.0926 9	33.5604 6	34.9935 4
Improvement in power	34.1%	28.4%	28.7%	31.3%

Table 4. Average power without, with MPPT and improvement in power.

From table we get the improvement in power is better at M1 (34 %) but at M2, M3 equal 28 % and at M4 (31 %). Then we concluded that for MPPT we get maximum power depends on the step size of perturbation M.

**B. The output power at P&O-3 test**

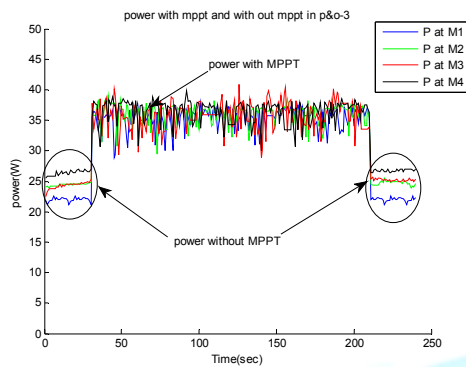


Figure 16. The output power at P&O-3 test

From figure 16, we get the maximum power occurs at M4 ( $P_{MAX} = 36.52983W$ ) but at M1,  $P_{MAX} = 35.02486W$ . Also table 5, show the average output power without MPPT, the average power with MPPT and the improvement in output power at different step values of perturbation M1, M2, M3 and M4.

P&O-3	M1 0.01	M2 0.001	M3 0.05	M4 0.005
Average power without MPPT	21.13630	24.60713	24.83051	26.57616
Average power with MPPT	35.21408	35.81751	35.80108	36.41396
Improvement in power	40.0%	31.3%	30.6%	27.0%

Table 5. Average power without, with MPPT and improvement in power.

C. The output power at INC test

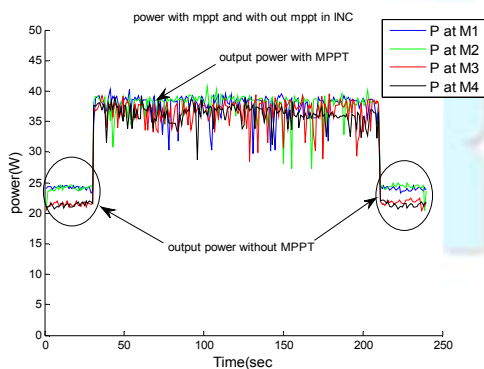


Figure 17. The output power at INC test

From figure 17, we get improvement in MPPT due to using the algorithm of INC comparing with the P&O algorithms, also we get at M1  $P_{MAX} = 37.47989W$  and at M4  $P_{MAX} = 35.627W$ . Also table 6, show the average output power without MPPT, the average power with MPPT and the improvement in output

power at different step values of perturbation M1, M2, M3 and M4.

INC	M1 0.01	M2 0.001	M3 0.05	M4 0.005
Average power without MPPT	24.05272	24.24319	21.64081	21.71165
Average power with MPPT	37.49398	37.77316	36.69017	36.18164
Improvement in power	35.8%	35.8%	41.0%	40.0%

Table 6. Average power without, with MPPT and improvement in power.

6. Comparison between different algorithms at different tests

Table 7 show comparison between different algorithms at different tests for the average output power without MPPT, the average power with MPPT, the improvement in output power at different step values of perturbation M1, M2, M3 and M4.

P&O-1	M1 0.01	M2 0.001	M3 0.05	M4 0.005
Average power without MPPT	23.62375	24.4210	23.92410	24.03029
Average power with MPPT	35.85759	34.09269	33.56046	34.99354
Improvement in power	34.1%	28.4%	28.7%	31.3%
P&O-3	M1 0.01	M2 0.001	M3 0.05	M4 0.005
Average power without MPPT	21.13630	24.60713	24.83051	26.57616
Average power with MPPT	35.21408	35.81751	35.80108	36.41396
Improvement in power	40%	31.3%	30.6%	27%
INC	M1 0.01	M2 0.001	M3 0.05	M4 0.005
Average power without MPPT	24.05272	24.24319	21.64081	21.71165
Average power with MPPT	37.49398	37.77316	36.69017	36.18164
Improvement in power	35.8%	35.8%	41%	40%

Table 7. Comparison between different algorithms at different tests

7. Conclusions

The photovoltaic cell characteristics are measured and plotted in the actual environmental and simulated with MATLAB to show the effects of irradiance and temperature on the operation of the photovoltaic array. High efficiency control and measurement circuit of MPPT algorithms are implemented using PIC microcontroller to study the actual behavior of

MPPT algorithms and compared the two algorithms at different step size values of perturbation. Experimental results showed that the best value of step size of perturbation in P&O and INC algorithms is in the range between 0.01 and 0.005. The INC algorithm improves the limitations of the P&O algorithm by improving the tracking accuracy and dynamic performance under atmospheric rapidly varying conditions.

### 8. References

- 1- B. Subudhi, and R. Pradhan, "A Comparative Study on Maximum Power Point Tracking Techniques for Photovoltaic Power Systems", IEEE Transactions on Sustainable Energy, vol. 57, issue 1, pp. 89-98, July 2012.
- 2- Tat Luat Nguyen and Kay-Soon Low, "A Global Maximum Power Point Tracking Scheme Employing DIRECT Search Algorithm for Photovoltaic Systems", IEEE Transactions on Industrial Electronics, vol. 57, no. 10, pp. 3456-3467, October 2010.
- 3- E. Koutroulis and F. Blaabjerg, "A New Technique for Tracking the Global Maximum Power Point of PV Arrays Operating Under Partial-Shading Conditions", IEEE Transactions on Industrial Electronics, vol. 2, no. 2, pp. 184-190, April 2012.
- 4- Sairaj V. Dhople, Ali Davoudi, Alejandro D. Domínguez-García, and Patrick L. Chapman, "A Unified Approach to Reliability Assessment of Multiphase DC-DC Converters in Photovoltaic Energy Conversion Systems", IEEE Transactions on Power Electronics, vol. 27, no. 2, pp. 739-751, February 2012.
- 5- Hoonki Kim, Sangjin Kim, Chan-Keun Kwon, Young-Jae Min, Chulwoo Kim and Soo-Won Kim, "An Energy-Efficient Fast Maximum Power Point Tracking Circuit in an 800 $\mu$ W Photovoltaic Energy Harvester " IEEE Transactions on Power Electronics, vol. 28, issue 6, pp. 2927-2935 October 2012.
- 6- Neil S. D'Souza and Luiz A.C. Lopes, "Comparative study of variable size perturbation and observation maximum power point trackers for PV systems ", IEEE Transactions on Industrial Electronics, vol. 80, issue 3, pp. 296-305, March 2010.
- 7- R. Mostafa, A. Razek, E. Faure, "Optimum operation of a Photovoltaic energy conversion system". 18th Electrical Power conference, UPEC 83, England, 11-13, pp. 387-392, April 1983,
- 8- S. Ozcelik, H. Prakash and R. Chaloo "Two-Axis Solar Tracker Analysis and Control for Maximum Power Generation", Elsevier, Procedia Computer Science, vol. 6, pp. 457-462, 2011.
- 9- Jen-Cheng Wang, Jyh-Cherng Shieh and Joe-Air Jiang "A Novel Method for Determination of Dynamic Resistance for Photovoltaic Modules", Elsevier, Energy, vol. 36, pp. 5968-5974, 2011.
- 10- Bidyadhar Subudhi, and Raseswari Pradhan, "A Comparative Study on Maximum Power Point Tracking Techniques for Photovoltaic Power Systems", IEEE Transactions on Sustainable Energy, vol. 4, no. 1, pp. 89-98, January 2013.
- 11- Badia Amrouche , Abderrezak Guessoum and Maiouf Belhmel, "A simple behavioral model for solar module electric characteristics based on the first order system step response for MPPT study and comparison", Elsevier Applied Energy, vol. 91, pp. 395-404, 2012.
- 12- Chia Seet Chin, Soo Siang Yang and Kenneth Tze Kin Teo "Maximum Power Point Tracking for PV Array under Partially Shaded Conditions", Third International Conference on Computational Intelligence, Communication Systems and Networks, IEEE, pp. 72-77, 2011.
- 13- D. Sera, T. Kerekes, R. Teodorescu, and F. Blaabjerg, "Improved MPPT method for rapidly changing environmental conditions," In Industrial Electronics, IEEE International Symposium on, vol. 2, pp.1420-1425. 2006.
- 14- D. Sera, T. Kerekes, R. Teodorescu, J. Hantschel , and M. Knoll, "Optimized Maximum Power Point Tracker for Fast-Changing Environmental Conditions" IEEE Transactions on Industrial Electronics, vol. 55, no. 7, July 2008.
- 15- Mei Shan Ngan, Chee Wei Tan, " A Study of Maximum Power Point Tracking Algorithms for Stand-alone Photovoltaic Systems ", IEEE Applied Power Electronics Colloquium (IAPEC), Johor Bahru, pp. 22-27, April 2011.
- 16- Fangrui Liu and et, "A Variable Step Size INC MPPT Method for PV Systems" IEEE Transactions on Industrial Electronics, vol. 55, no. 7, July 2008.
- 17- A. Chikh and A. Chandra, " An optimum Method for Maximum Power Point Tracking in Photovoltaic Systems", IEEE Power and Energy Society General Meeting, San Diego, CA, pp. 1-6, July 2011.
- 18- M. Jantsch, M. Real and et." Measurement of PV Maximum Power Point Tracking Performance" International Electrotechnical Commission

contact: Netherlands Energy Research Foundation  
ECN, P.O. Box 1, NL-1755 ZG Petten.

- 19- M.A. Farahat, H.M.B. Metwally and Ahmed A. Mohamed, "Optimal choice and design of different topologies of DC-DC converter used in PV systems, at different climatic conditions in Egypt", Renewable Energy, vol. 43, pp. 393-402, 2012.
- 20- Islam M. R., Young uang and et," Simulation of PV Array Characteristics and Fabrication of Microcontroller Based MPP", International Conference on Electrical and Computer Engineering (ICECE), pp. 155-158, Dhaka, 2010.

**Fathy M. Mustafa:** received the B.Sc. degree in Electronics and communications department from the Faculty of Engineering, Fayoum University, Fayoum, Egypt, in 2003. He is earned the M.Sc degree in Electronics and communication engineering in 2007 from Arab Academy for Science and Technology & Maritime Transport College of Engineering and Technology, Alexandria, Egypt. He received his Ph.D in electrical engineering from Mina University in 2013. Her areas of interest include optical communications, optical amplifiers and solar cells.

**M. Elzalik:** received the B.Sc. degree in Process Control Technology department from the Faculty of industrial Education, Beni-suef University, Beni-suef, Egypt, in 2007. He is earned the M.Sc degree in Electrical Power and Machines in 2013 from Faculty of Industrial Education, Suez University, and Suez, Egypt. His areas of interest include renewable energy, power electronics, and electrical machines.

**R. Mostafa:** Professor in Process Control Technology department from the Faculty of industrial Education, Beni-suef University, Beni-suef, Egypt.

The logo for IJREAT PRDGG features a stylized globe in the background. The word 'IJREAT' is written in a large, light blue, sans-serif font across the middle of the globe. Below the globe, the word 'PRDGG' is written in a larger, bold, light blue, sans-serif font.